PHYSIOLOGIA PLANTARUM 100: 729–738. 1997
Printed in Denmark – all rights reserved

ISSN 0031-9317

Infrared microspectroscopy: Sampling heterogeneity in plant cell wall composition and architecture

M. C. McCann, L. Chen, K. Roberts, E. K. Kemsley, C. Sene, N. C. Carpita, N. J. Stacey and R. H. Wilson

McCann, M. C., Chen, L., Roberts, K., Kemsley, E. K., Sene, C., Carpita, N. C., Stacey, N. J. and Wilson, R. H. 1997. Infrared microspectroscopy: Sampling heterogeneity in plant cell wall composition and architecture. – Physiol. Plant. 100: 729–738.

The use of probes such as monoclonal and polyclonal antibodies to specific cell wall components, at both the light and electron microscope levels, has demonstrated the diversity in cell wall composition between species, between tissues, between different regions of the cell surface, and even within a single wall. Traditional methods of cell wall analysis have provided valuable information on wall composition and architecture, but, by having to rely on the use of bulk samples, have averaged out this intrinsic heterogeneity. Fourier Transform Infrared (FTIR) microspectroscopy addresses this problem by providing chemical information from an area as small as 10×10 μm of a single cell wall fragment or area of a tissue section that has been imaged with a microscope accessory.
We have used FTIR microspectroscopy as a powerful and extremely rapid assay for wall components and putative cross-links in muro. The spectra are sensitive to polymer conformation, and the use of polarisers in the microscope accessory allows the orientation of particular functional groups to be determined, with respect to the long axis of elongating cells. The spectra constitute species and tissue-specific 'fingerprints', and the use of classical discriminant analysis may provide the opportunity for correlating spectral features with chemical, architectural or rheological wall properties. Spectral mapping of an area of a specimen allows the morphological features resulting from cell growth and differentiation to be characterised chemically at the single cell level.

Key words – Cell wall architecture, elongation, Fourier Transform Infrared spectroscopy, functional group mapping, hydration, microspectroscopy, pectin, polarised IR spectroscopy, principal component analysis.

M. C. McCann (corresponding author, e-mail maureen.mccann@bbsrc.ac.uk), K. Roberts and N. J. Stacey, Dept of Cell Biology, John Innes Centre, Colney Lane, Norwich, NR4 7UH, UK; L. Chen, School of Physics, Univ. of East Anglia, Norwich, NR4 7TJ, UK; E. K. Kemsley and R. H. Wilson, Dept of Food Biophysics, Inst. of Food Research, Colney Lane, Norwich, NR4 7UA, UK; C. Sene, Dow Corning Europe, Parc Industriel, B-7180 Seneffe, Belgium; N. C. Carpita, Dept of Botany and Plant Pathology, Purdue Univ., West Lafayette, IN 47907, USA.

FTIR spectroscopy and plant cell walls

Longitudinal and transverse sections of plant parts, stems, roots, or leaves, provide a developmental snapshot of cell growth and differentiation. In the light microscope, the use of probes, such as monoclonal antibodies coupled to fluorescent markers, has revealed the tissue-specific distributions of particular cell wall components in transverse sections of plant materials (Knox et al. 1990, Pennell and Roberts 1995) whilst longitudinal sections reveal developmental regulation of those components. For example, Fig. 1 A,B shows that a carbohydrate epitope on an arabinogalactan protein is restricted to guard cells in the epidermis of *Zinnia* leaves, whilst methyl-esterified pectin is present in all of the epidermal cell walls. In the electron microscope, two neighbouring tomato cells of the same tissue type can have very different cell surface composition during fruit ripening (Fig.

Received 26 March, 1997

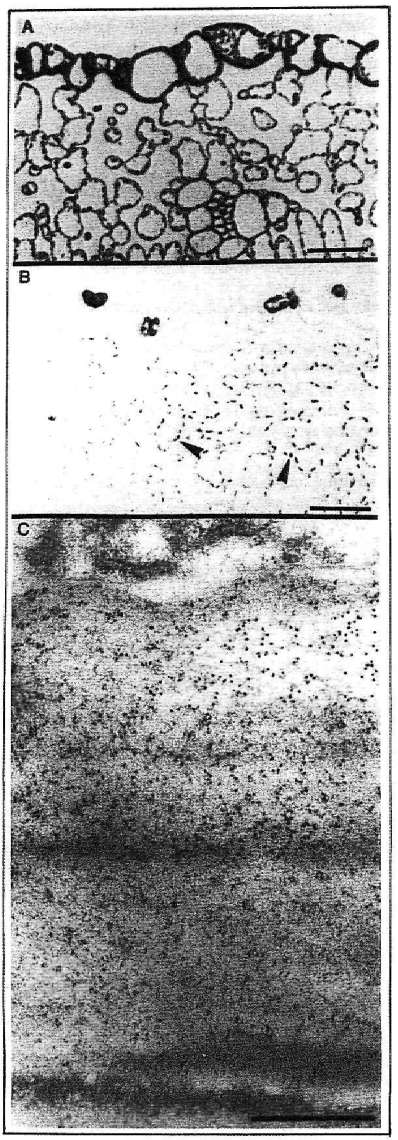

Fig. 1. Light micrographs of 1 μm sections of *Zinnia* leaves which have been immunogold-labelled and silver-enhanced. Immunolabelled material appears black using bright-field microscopy, but the spotty staining inside the cells is an artefact as a result of precipitation of silver grains on the chloroplasts (indicated by arrows). (A) JIM 7, a monoclonal antibody that recognises a relatively methyl-esterified pectic epitope, labels all cell walls in the leaf. (B) JIM 13, a monoclonal antibody that recognises a carbohydrate epitope on an arabinogalactan protein, labels guard cells in the epidermis. Scale bars in A and B represent 75 μm. (C) In pericarp cell walls of orange tomatoes, labelling with the JIM 5 antibody that recognises a relatively unesterified pectic epitope, shows that the pectin within the wall of one cell has undergone de-esterification, while domains of the neighbouring cell wall remain methyl esterified. Scale bar represents 500 nm.

1C) (Steele et al. 1997). Dissection of a particular cell type at a particular developmental stage is seldom practical for chemical analysis, which requires microgram to milligram quantities of material. Thus, traditional methods of cell wall chemistry average out the intrinsic heterogeneity of the plant extracellular matrix (McCann et al. 1995).

Gas chromatography-mass spectroscopy (GC-MS) is the most widely used technique for carbohydrate analysis of cell walls, providing information on the sugar composition and the glycosidic linkages of the polymers. Isolated polysaccharides or cell walls are first methylated, and then hydrolysed to monosaccharides and derivatised to volatile alditol acetates, that can be separated and identified by gas chromatography. Linkage structure is deduced from characteristic molecular fragmentation patterns of the partially-methylated derivatives (Carpita and Shea 1989). This has provided valuable information on polysaccharide chemistry but we also require methods of analysis that can probe the wall without modifications to cell wall architecture by preparative treatments, to examine polymer conformations, orientations, and interactions in situ. Spectroscopies including nuclear magnetic resonance (NMR) spectroscopy (Foster et al. 1996, Ha et al. 1996), Fourier Transform Infrared (FTIR) and FT-Raman offer this opportunity (McCann et al. 1992, Sene et al. 1994). For homogeneous bulk sampling, NMR spectroscopy is used to probe wall chemical composition, orientation of polymers, relative mobility of polymers in solution, and even how polymers interact with each other. Ideally though, we would like to obtain chemical information from single cell walls.

New microspectroscopic techniques allow us to probe micro-heterogeneity in samples, non-invasively, obtaining chemical information from picogram or even femtogram quantities of material. The coupling of an FTIR spectrometer to an appropriate microscope allows selection of a particular area (as small as 10 μm × 10 μm) in any field of view for microsampling, whilst Raman microscopes have a resolution of 1 μm × 1 μm. However, we have found that many primary cell walls (thin walls deposited during growth) are not good Raman scatterers, meaning that the Raman signal is too weak to provide good quality spectra of single cell walls. Secondary cell walls (thick walls deposited after cell growth has ceased) which predominate in woods are very suitable substrates for Raman microscopy (Atalla 1987). In this review, we will focus on the application of FTIR microspectroscopy to primary cell walls (McCann et al. 1992, 1993, 1994, 1995, Kemsley et al. 1994, Sene et al. 1994) including the spectral fingerprinting of cell walls and their component molecules, functional group mapping of an area of a sample, defining the orientation of macromolecules by polarised FTIR microspectroscopy, and identifying chemical differences between samples by digital subtraction or between groups of samples by principal component analysis. By relating optical images of the specimen to chemical information from IR spectroscopy, we

can begin to characterise changes in cell wall architecture during cell growth and differentiation at the single cell level.

A microscope accessory for the FTIR spectrometer

The energy of molecular vibrations corresponds to the infrared region of the electromagnetic spectrum. Complex molecules have a large number of vibrational modes associated with vibrations of specific bonds or functional groups including rocking, twisting, wagging, stretching and bending. In the IR spectrometer, an infrared source emits radiation with a range of frequencies (400 to 4 000 wavenumbers, measured in units of cm^{-1}) which is then passed through the sample. IR radiation is absorbed when the oscillating dipole moment due to a molecular vibration interacts with the oscillating electric vector of the IR beam in the spectrometer. This interaction will occur only if the vibration has an associated change in the dipole moment: the bond must be asymmetric (Williams and Fleming 1980). Particular chemical bonds in the sample will thus absorb radiation of specific frequencies from the beam, which passes to a detector.

The spectrometer is based on the optical design of the Michelson interferometer (Fig. 2). The IR beam from a conventional IR source is split into two paths. In one path, the beam is reflected by a fixed-position mirror where it is partially reflected to the source and partially transmitted to the detector. In the other leg of the interferometer the beam is also reflected, this time by a movable mirror that can be translated back and forth without tilt or wobble. The energy that reaches the detector is the sum of these two beams – both partially transmitted by the beam-splitter. The optical path difference gives reinforcement for an integral multiple of wavelengths ($n\lambda$) of the emitting source and destructive interference for $(n+1/2)\lambda$ as the mirror is moved. In a conventional infrared instrument, each frequency is passed through the sample and detected singly, but in an FT instrument, all of the frequencies are scanned simultaneously, speeding up data acquisition times from hours to minutes. The resulting interferogram can be described as an infinitely long cosine wave: for more than one frequency, the interferogram is the sum of the cosine waves of all the frequencies present in the source. It is the interferogram (intensity vs time) that is measured physically but the spectroscopist is more generally interested in the spectrum (intensity vs frequency). The interferogram and the corresponding spectrum are mathematically related to each other by a Fourier Transformation.

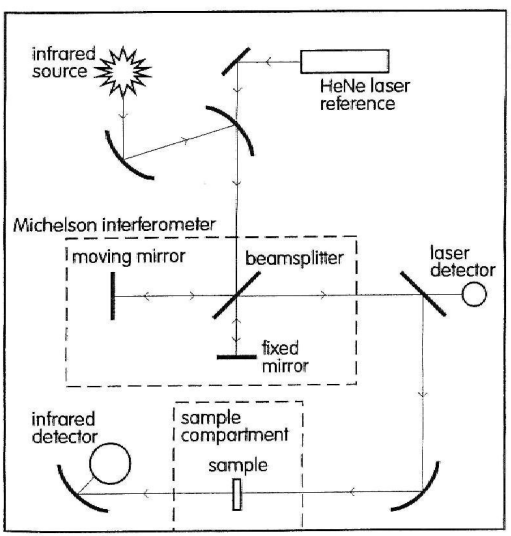

Fig. 2. Diagram of an FTIR spectrometer.

The two advantages of this approach for microspectroscopy are (1) the absence of slits and dispersing optics increases the energy arriving at the sample and (2) each interferogram, and therefore each spectrum, is generated rapidly (< 1 s) such that many spectra can be co-added in a short acquisition time to yield a spectrum with improved signal-to-noise ratio. Thus, the energy inefficiency of diverting the beam over an extended path through a microscope accessory can be tolerated (Perkins 1987). In addition, the tracking of the moving mirror position with a He-Ne laser (Fig. 2) produces a spectrum with a highly reproducible frequency scale, allowing digital subtraction of spectra (Wilson 1990). Glass absorbs in the IR region and so the beam is passed by a system of mirrors to a sample mounted on a barium fluoride window (an IR-transparent material) on the microscope stage and then by a special mirrored objective lens (Cassegrainian lens) to the detector. The white light for viewing the sample and the infrared light for obtaining the spectrum are both colinear and parfocal and so the area of a single cell wall from which IR data is obtained, including the cell type and its relative axial orientation, can be defined precisely. A four-blade rectangular aperture is inserted into the system and the blades adjusted to mask off the area of interest to a diffraction limit of 10 μm by 10 μm. With smaller aperture sizes, the wavelength of the radiation approaches the aperture size and the energy does not pass through the aperture.

Figure 3 shows isolated cell wall fragments, obtained by grinding onion parenchyma tissue in a mortar and pestle. The black box represents an area of 10 μm by 10 μm from which the spectrum was obtained in less than a minute. In the mid-IR spectrum, saturated esters absorb at 1740 cm^{-1} and unsaturated esters at 1720 cm^{-1} (Morikawa et al. 1978), amide-stretching bands of protein occur at 1650 and 1550 cm^{-1} (Sutherland 1952), carboxylic acid groups absorb at 1600 and 1414 cm^{-1} (Morikawa et al. 1978), phenolics at 1620 and 1515 cm^{-1} (Williams and Fleming 1980), and carbohydrates absorb between 1200 and 900 cm^{-1} (Williams and Fleming 1980). Below 1500 cm^{-1}, in the so-called 'fingerprint'

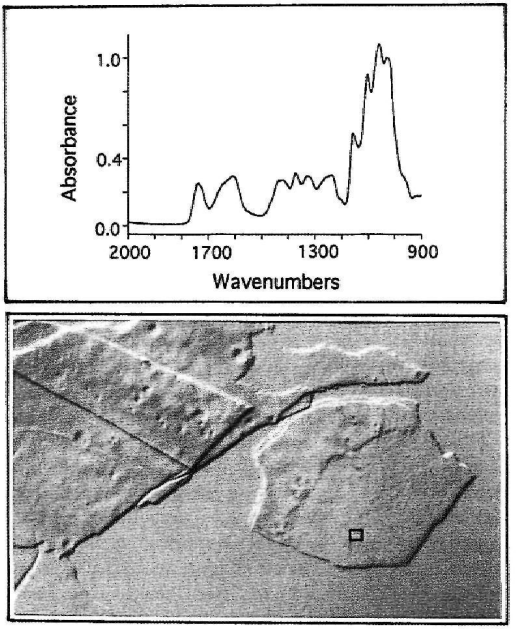

Fig. 3. A Fourier Transform Infrared (FTIR) spectrum obtained from the area marked on the light micrograph below of single cell wall fragments prepared from onion parenchyma tissue.

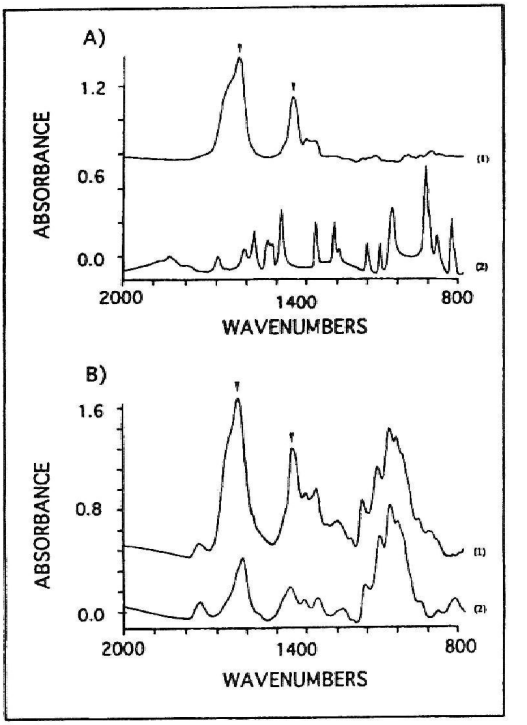

Fig. 4. FTIR spectra of pure CDTA (A, 1), pure imidazole (A, 2), and rice cell walls after extraction with CDTA (B, 1) and imidazole (B, 2). CDTA has strong absorbances at 1600 and 1406 cm^{-1} and these bands can be seen in the spectrum of CDTA-extracted cell wall material, even after extensive dialysis. The spectrum of imidazole-extracted cell wall material is free from any interferences from imidazole.

region, peaks cannot be readily assigned to particular vibrations because many complex vibrational modes overlap in this region. However, this region can be used to identify a compound or mixture of compounds from the characteristic spectral envelope.

A rapid method to check sample purity and homogeneity

The rapidity of spectral acquisition (1 to 2 min per spectrum) makes FTIR spectroscopy very useful for routine checking of sample purity or contamination. For example, pectins can be extracted from cell walls by extractants that chelate calcium ions such as cyclohexane *trans*-1,2-N,N,N',N'-diaminotetraacetate (CDTA) (Redgwell and Selvendran 1986) or imidazole (Mort et al. 1991). CDTA has strong absorbances at 1600 and 1406 cm^{-1} and these bands can be seen in the spectrum of CDTA-extracted cell wall material even after extensive dialysis (Fig. 4A1,B1). However, no contribution to IR spectra from imidazole can be detected after dialysis (Fig. 4A2,B2). By sugar analysis, it has been shown that imidazole extracts an equivalent pectic fraction (Mort et al. 1991) and is thus a more suitable chelating agent for vibrational spectroscopy.

Plant cell walls contain a great variety of polymers of different types (proteins, aromatics, polysaccharides), each having a particular molecular conformation and interacting with neighbouring molecules in a specific way (McCann and Roberts 1991, Carpita and Gibeaut 1993). This complexity appears in the vibrational spectra of the cell walls, with subtle variations in intensity or absence of some bands in the spectrum reflecting compositional differences. We have compared FTIR spectra from the cell walls of five plants, one dicotyledon, one non-graminaceous monocotyledon, and three graminaceous monocotyledon species (Sene et al. 1994). It is possible to differentiate between the two non-gramineae and the three gramineae species from broad characteristics, particularly from bands associated with pectins and proteins. This is a consequence of the very different cell wall composition of the Poaceae (Carpita and Gibeaut 1993). However, all the spectra are distinctive (Fig. 5). For example, in the spectra of rice and sweetcorn, peaks at 1600 and between 1160 and 970 cm^{-1} have different line-shapes and intensity (Sene et al. 1994). These variations are sufficient for spectral discrimination.

A further use of fingerprinting is in detecting modifications to cell walls, either as a consequence of muta-

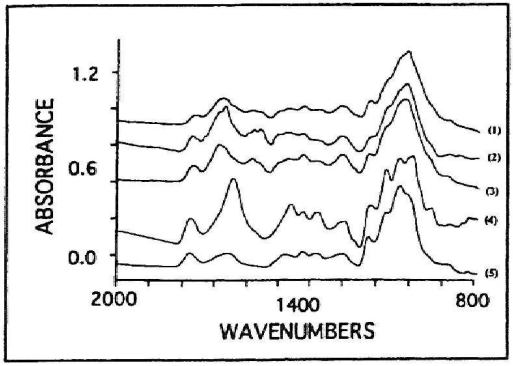

Fig. 5. FTIR spectra of cell walls isolated from parenchymatous tissues of polypogon (1), rice (2), sweet corn (3), carrot (4) and onion (5). Each cell wall gives a characteristic spectrum that can be used as a fingerprint for a given cell wall.

tion, transformation or environmental adaptation. The FTIR spectrum obtained from walls from suspension-cultured cells of tomato (Fig. 6A) is similar to that from the onion parenchyma cell wall (both contain cellulose, hemicellulose and pectin) (Fig. 6C) although there is clearly more protein in the tomato walls (amide stretches at 1550 and 1650 cm^{-1}). When suspension-cultured cells of tomato are adapted to growth on a cellulose synthesis inhibitor, 2,6-dichlorobenzonitrile (DCB), they make a pectin-rich wall that lacks a cellulose-xyloglucan network (Shedletzky et al. 1990). The spectrum of the DCB-adapted tomato cell walls (Fig. 6B) more closely resembles that of either purified pectins or of a commercial polygalacturonic acid sample from Sigma (Fig. 6D) with peaks in common at 1140, 1095, 1070, 1015 and 950 cm^{-1} in the carbohydrate region of the spectrum, as well as the free acid stretches at 1600 and 1414 cm^{-1} and an ester peak at 1725 cm^{-1}. An ester band at 1740 cm^{-1} is evident in both onion parenchyma and non-adapted cell wall samples. It is possible that this shift in the ester peak simply reflects the different local molecular environment of this bond, but it is also possible that a different ester is made in the adapted cell walls, as phenolic esters absorb around 1720 cm^{-1} whilst carboxylic esters absorb at 1740 cm^{-1}. The carboxylic acid stretches at 1600 and 1414 cm^{-1} are more prominent in the adapted walls, indicating a much higher proportion of unesterified pectin in these walls. These results are consistent with chemical analyses which indicate that unadapted walls contain about 20% uronic acid, whereas in adapted walls this component rises to about 40–45% of the dry weight (Wells et al. 1994). There are three advantages of using FTIR microspectroscopy in this instance: firstly, the rapidity of assaying wall adaptation; secondly, the spectra are non-biased and all major chemical changes are shown; thirdly, microsampling of different areas of the sample ensures that the observed changes are representative of the entire cell population.

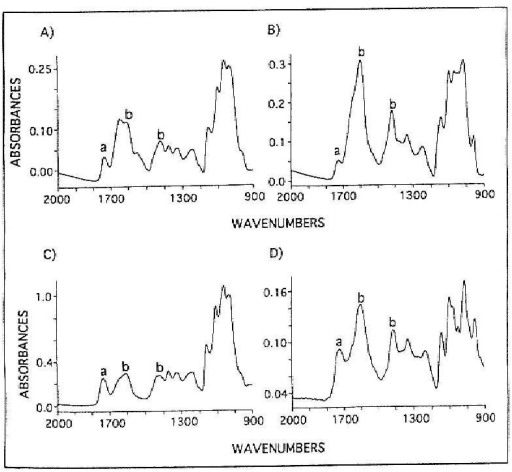

Fig. 6. FTIR spectra of walls of (A) non-adapted tomato suspension cells and (B) DCB-adapted tomato suspension cells, (C) onion parenchyma cell walls, and (D) polygalacturonic acid (Sigma). a = ester peak, b = free acid stretches from pectins.

Digital subtraction of FTIR spectra reveals the differences between them

One of the most useful features of the spectra is that digital subtraction can be applied to see clearly the differences between two spectra. Absorbance readings vary between spectra since the total absorbance depends on the thickness of the sample in the path of the beam and this is difficult to control rigorously. Before digital subtraction, therefore, one spectrum is scaled relative to the other by an appropriate subtraction factor.

One of the most common modifications to pectins is methyl esterification of the carboxylic acid functional groups that removes the negative charges used for calcium cross-linking. In walls of tobacco suspension cells, the proportion of total esters is initially about 50% in dividing cells, rises to 78% during maximal elongation and then drops to 68% at stationary phase after elongation has stopped (McCann et al. 1994). These changes in esterification are easily assayed by FTIR spectroscopy. Figure 7 shows the spectra obtained from walls of cells in exponential cell division, maximally elongating and after elongation. The difference spectrum shows that there is a decrease in the proportion of unesterified pectin between maximal cell division and maximal cell elongation; the ester peak at 1740 has increased, whilst free acid stretches at 1600 and 1414 have decreased proportionally (Fig. 7). After elongation, the ester peak decreases relative to the free acid stretches which increase, indicating a rise in the proportion of relatively unesterified pectin between maximal elongation and stationary phases.

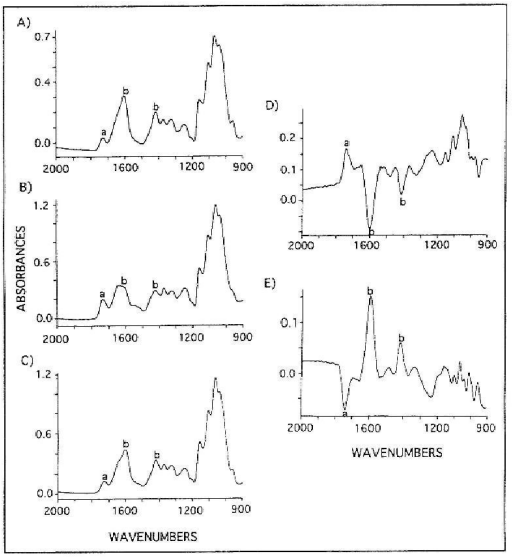

Fig. 7. FTIR spectra obtained from single wall fragments of suspension-cultured tobacco cells at different growth stages show that an increase in esterification of the wall occurs between 5 and 9 days during cell elongation and a decrease in esterification of the wall occurs between 9 and 16 days. (A) Spectrum of walls of 5-day-old (exponentially dividing) tobacco cells. (B) Spectrum of walls of 9-day-old (maximally elongating) tobacco cells. There is a change in the relative intensities of the ester band at 1740 cm^{-1} (labelled a) and the carboxylic acid stretches at 1600 and 1414 cm^{-1} (labelled b). (C) Spectrum of walls of 16-day-old (fully elongated) tobacco cells. (D) Difference spectrum generated by digital subtraction of spectrum (A) from spectrum (B) shows the increase in the ester band at 1740 cm^{-1} (labelled a) and the decrease in the carboxylic acid stretches at 1600 and 1414 cm^{-1} (labelled b). (E) Difference spectrum generated by digital subtraction of spectrum (B) from spectrum (C) shows the increase in free acid stretches at 1600 and 1414 cm^{-1} (labelled b) and the decrease in ester at 1740 cm^{-1} (labelled a). Some of the peaks in the carbohydrate region in spectrum (D) show inversion in spectrum (E) and are therefore possibly assignable to the ester group.

In contrast, the walls of tobacco cells adapted to grow on 0.5 *M* NaCl (Iraki et al. 1989a,b) show no change at equivalent growth stages apart from a substantial increase in protein and phenolic content by stationary phase. These cells expand isodiametrically at a very slow rate. FTIR difference spectra generated by digital subtraction of the spectra of unadapted tobacco cell walls from the spectra of NaCl-adapted tobacco cell walls at equivalent growth stages show that walls of adapted cells have more protein, saturated and phenolic esters (absorbances at 1740 and 1720 cm^{-1}) and unesterified pectin in a given area of cell wall (Fig. 8). A strong absorbance at 1620 cm^{-1} is also present in spectra of adapted cell walls which may be assigned as a phenyl conjugated C = C, such as occurs in all hydroxycinnamic acids and their esters.

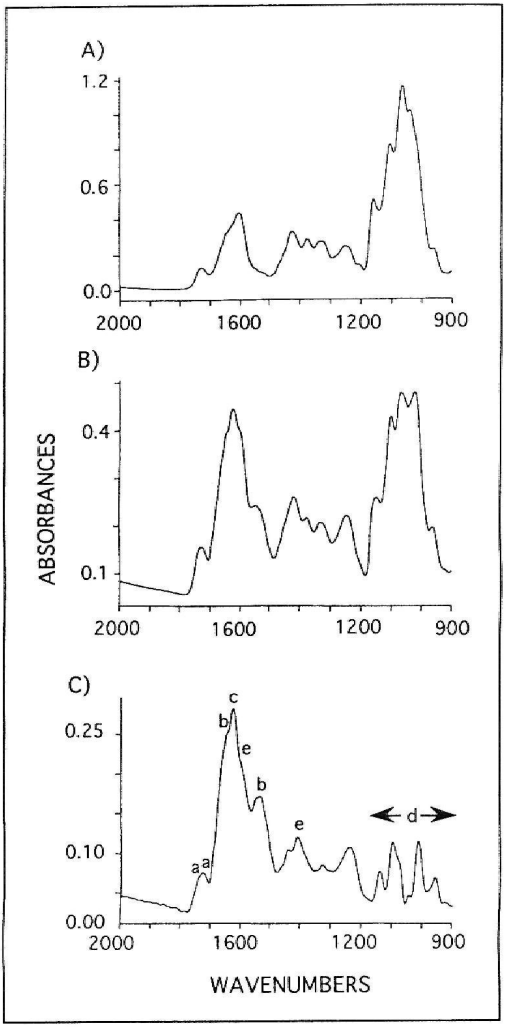

Fig. 8. (A) Spectrum of walls of 16-day-old (fully elongated) tobacco suspension-culture cells. (B) Spectrum of walls from 26-day-old NaCl-adapted tobacco suspension cultured cells, representing the equivalent growth stage. (C) Difference spectrum generated by digital subtraction of the spectrum of unadapted walls (16 days old) from the spectrum of NaCl-adapted walls (26 days old) at stationary phase. NaCl-adapted walls contain more protein (amide stretches at 1550 and 1650 cm^{-1}; labelled b), esters (a saturated ester stretch at 1740 cm^{-1} and a phenolic ester at 1720 cm^{-1}; labelled a), pectin (carboxylic acid stretches at 1600 and 1414 cm^{-1}; labelled e) and a 'fingerprint' in the 1200 to 900 cm^{-1} region of the spectrum (labelled d) characteristic of polygalacturonic acid (see Fig. 6D), and a band at 1620 cm^{-1} (assignable to a phenyl-conjugated C = C in, for example, ferulic esters; labelled c), in a given area of cell wall than in the same area of wall from unadapted cells.

Polarised FTIR spectroscopy can be used to examine macromolecular orientations

A further example of the use of digital subtraction is in the comparison of polarised spectra. Polarisers can be inserted in the path of the IR beam to determine whether band frequencies of specific functional groups are oriented transversely or longitudinally with respect to the long axis of the cell. Without changing the size or position of the aperture, the orientations of the two polarisers are changed. A separate background spectrum must be obtained at each orientation as the polarisers affect the energy throughput. The digital subtraction factor of the absorbance spectra is then unity.

Figure 9 shows the two spectra obtained from carrot stem epidermis with the polarisers parallel and perpendicular respectively to the long axis of the cell. The difference spectrum shows that an extreme case of polarisation of molecules exists in the epidermis with virtually every peak polarised including those associated with pectic polysaccharides and proteins. This may reflect the role of epidermal tissue that acts as a major constraint in organ growth. The tissue-specific differences in orientations of matrix components as well as cellulose indicate that architecture of walls as well as composition is heterogeneous (McCann et al. 1993).

A concern for us was that the orientations that we observed in these walls might be the consequence of looking at dried walls, where matrix polymers may have collapsed on to the cellulosic microfibrils. Therefore, we constructed a hydration cell in which wet samples, or samples of controlled moisture content could be analysed. The molecular orientations that we observed previously (McCann et al. 1993) were not affected by the hydration state. Using the hydration cell, it is now possible to investigate wet samples routinely, and we have observed that some cell walls exhibit greater spectral changes on dehydration than others, although the changes in the spectrum are generally slight.

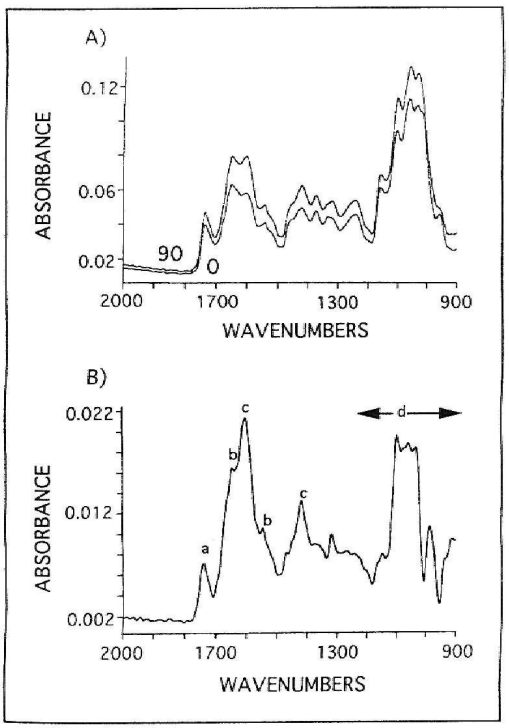

Fig. 9. (A) FTIR spectra of an area of epidermis from a 25 μm thick fresh section of stem of etiolated carrot seedling with polarisers aligned parallel and perpendicular to the direction of cell elongation. (B) The difference spectrum generated by digital subtraction shows almost every peak to be sharply polarised in the tissue – ester peak at 1740 cm^{-1} (a), protein peaks at 1650 and 1550 cm^{-1} (b), free acid peaks at 1600 and 1414 cm^{-1} (c), and a large number of absorbances in the carbohydrate region of the spectrum, 1200 to 900 cm^{-1} (d).

Principal component analysis (PCA) allows comparison of groups of spectra

Whilst digital subtraction allows deductions to be made from a single pair of spectra, it is frequently more useful to compare spectra in groups, and to be able to assign an unknown to a particular group. Parenchyma cell walls from ten different species of fruits and vegetables were examined using FTIR microspectroscopy (Kemsley et al. 1994). For nine species, a single fruit or vegetable was used. For the tenth, apple, samples from 10 individual fruits of the same variety were prepared. Visual examination suggests that there is more variation in the set of non-apple spectra than the apple spectra (Fig. 10A,B). In particular, the region 1500–1800 cm^{-1} containing bands arising from constituents including pectin and protein appears more variable inter-species than intra-species. This is confirmed by a more substantive assessment, made by comparing the variance spectra of the two data sets, obtained by calculating the variance of the absorbance values at each data point (Fig. 10C). By using an *F*-test on the ratio of variances in each data set, the null hypothesis that no spectral variation is caused by plant species can be rejected at the 0.1% level: the two data sets cannot be considered as arising from the same parent population.

This result can also be demonstrated by applying a multivariate statistical analysis to the spectra, showing that apple and non-apple spectra can be assigned into one of two groups, apple or non-apple, sufficiently well for no misclassification of an unknown to occur (Kemsley et al. 1994). To be able to classify spectra in groups, a data reduction technique, principal component analysis (PCA), is applied. A typical spectrum contains several hundred data points (or 'variates') but these variates will normally be correlated with one another, to a greater or lesser extent. Thus, in the example above, if most of the variability between spectra is accounted for by pectin

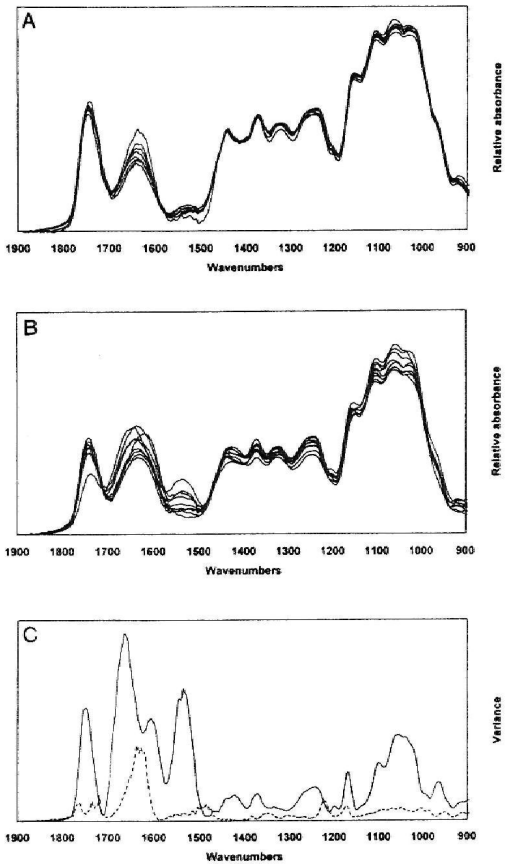

Fig. 10. (A) Area-normalized spectra of parenchyma cell walls from 10 different apples. (B) Area-normalized spectra of parenchyma cell walls from 10 species other than apple. (C) Variance spectra of the two data sets (-----), apple; (——), non-apple.

and protein, then a set of spectral points representing pectin will vary in a correlated fashion, and another set of spectral points representing protein will vary in a correlated fashion but independently of the former set. PCA removes the redundancy of having many points varying in a correlated way by transforming the original data into a set of new, uncorrelated variates, termed the principal component (PC) scores. In doing so, a rearrangement takes place, such that only the first few scores are required to describe the information contained in the many original variates (Lai et al. 1994). In the example above, the groups of apple and non-apple spectra were relatively easy to distinguish by eye, but PCA can distinguish very subtle spectral changes. Of course, the greater the group sizes, the more confidence can be placed in the group classifications, and the more robust will be any model established for the classification of an unknown.

An example of the use of PCA to discriminate between two groups which vary non-predictably in their spectral characteristics is discussed below.

Whilst suspension culture systems provide some information about correlations between cell wall modifications and cell growth and development, mutant phenotypes are an essential requirement to study any correlation rigorously. Screening for cell wall mutants is a laborious process as phenotypes are rarely predictable and assays are time-consuming. A large screen for cell wall mutants conducted by Prof Chris Somerville's group, focussed on identifying variations in the amount of neutral cell wall sugars by GC-MS analysis, and took many years (Reiter et al. 1993). Using this group of mutants, and through a collaboration with Dr Wolf-Dieter Reiter, State Univ. of Connecticut, we obtained triplicate-averaged and baseline-corrected FTIR spectra from freeze-dried leaves of 20 wild-type and 34 mutant *Arabidopsis* plants. The plants were grown in the dark for two days prior to harvesting to de-starch the leaves, which were then washed in ethanol to remove chlorophyll, freeze-dried and an area of the leaf selected away from the mid-rib and other veins for spectral collection. Different leaves from the same plant showed very minor spectral differences, but differences between mutant and wild-type plants were significant, with the calculated variance of spectra from mutant leaves being six times greater than that of spectra from wild-type leaves. A PCA plot of the spectra using the first two PC scores (accounting for most of the variability between spectra) shows a clear discrimination between mutant and wild-type leaves (Fig. 11). One mutant was classified as wild type, but this turned out to be a mutant altered in

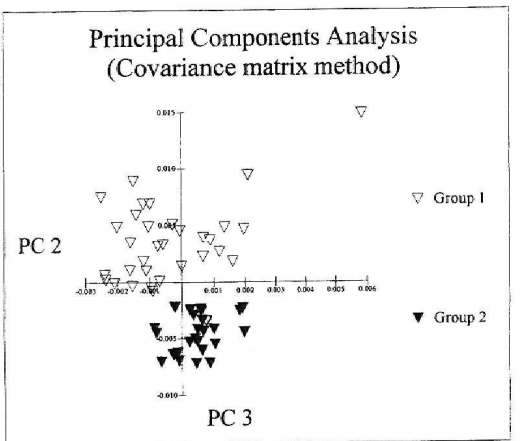

Fig. 11. Principal component analysis of FTIR spectra distinguishes between mutant (Group 1) and wild-type (Group 2) *Arabidopsis* leaves. One mutant, Fah 1, was mis-classified as wild type, but this mutant is distinguished from the others in being a phenolic rather than neutral sugar mutation (Chapple et al. 1992, Reiter et al. 1993).

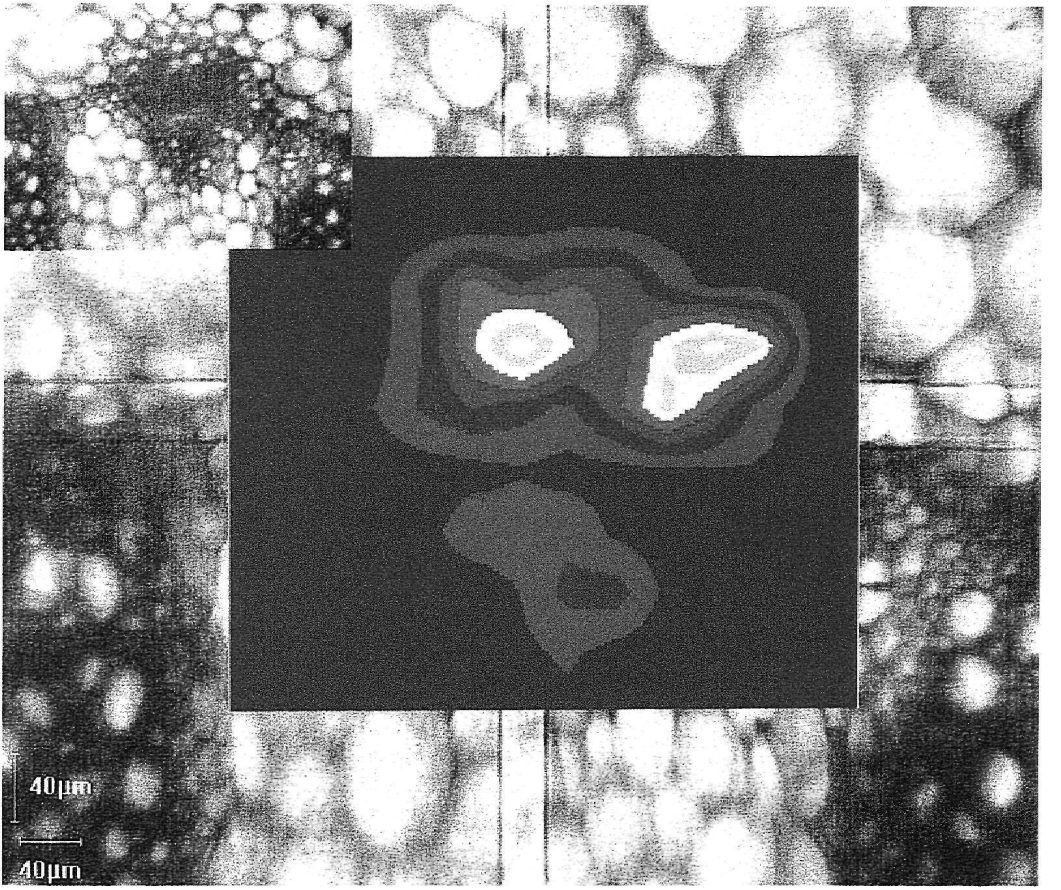

Fig. 12. A functional group map of the distribution of absorbance in the ester peak at 1740 cm^{-1} ratioed to the carboxylic acid peak at 1600 cm^{-1} over an area of stem section of *Zinnia elegans*. In the colour map, blue represents low ratioed absorbance intensity, and white, high ratioed absorbance intensity. The inset picture of the section shows the morphological features corresponding to areas of high ester intensity.

lignin rather than wall carbohydrate composition (Chapple et al. 1992). FTIR spectroscopy may prove to be a rapid means of screening for cell wall mutants, in particular for pectin mutants, as the free acid and ester peaks are well-resolved in the spectrum. These preliminary studies using PCA indicate that we may be able to correlate spectral features with chemical or biophysical properties of cell walls in instances where assignments for specific peaks are difficult to make, and thus begin to generate predictive models.

Making spectral maps of an imaged area

In plant organs, the presence of growth gradients and different tissue types mean that spectral mapping of the entire organ is very desirable. Using a motorised X-Y stage, an area from a transverse or longitudinal section can be mapped at 5- to 10-µm intervals. Collection of hundreds of complete spectra takes a few hours, and the data can then be displayed as a series of functional group plots of the area mapped by aligning the infrared map with the light micrograph of the sample. Current software packages permit single peaks to be selected for display, or, more usefully to overcome the problem of variability in section thickness, a ratio of one peak to a chosen reference peak. An example of the distribution of the ester peak at 1740 cm^{-1} ratioed to the carboxylic acid peak at 1600 cm^{-1} in a section of stem from *Zinnia elegans*, reveals that relatively more esterified pectin is localised in the vascular bundles (Fig. 12). The collection of such maps provides the closest correspondence between the visible micro-heterogeneity of the plant extracellular matrix and the chemical and architectural changes that occur in it during cell growth and differentiation.

Acknowledgments – M. C. M is funded by a Royal Society University Research Fellowship held through the University of East Anglia. R. H. W., E. K. K., K. R., and N. J. S. gratefully acknowledge the financial support of the BBSRC. L. C. acknowledges a Norwich Research Park studentship award, and C. S. was funded by an EC FLAIR programme. N. C. C. acknowledges financial support from grant No. 96-35304-3708 from the US Dept of Agriculture. Many thanks to Sue Bunnewell for photographic assistance.

References

Atalla, R. H. 1987. Raman spectroscopy and the Raman microprobe – valuable new tools for characterizing wood and wood pulp fibers. – J. Wood Chem. Technol. 7: 115–131.

Carpita, N. C. & Gibeaut, D. M. 1993. Structural models of primary cell walls in flowering plants: Consistency of molecular structure with the physical properties of the walls during growth. – Plant J. 3: 1–30.

– & Shea, E. M. 1989. Linkage structure by gas chromatography-mass spectrometry of partially-methylated alditol acetates. – *In* Analysis of Carbohydrates by GLC and MS (C. J. Biermann and G. D. Mc Ginnis, eds), pp. 155–216. CRC Press, Boca Raton, FL. ISBN 0-7923-3363-2.

Chapple, C. C. S., Vogt, T., Ellis, B. E. & Somerville, C. R. 1992. An *Arabidopsis* mutant defective in the general phenylpropanoid pathway. – Plant Cell 4: 1413–1424.

Foster, T. J., Ablett, S., McCann, M. C. & Gidley, M. J. 1996. Mobility-resolved ^{13}C-NMR spectroscopy of primary plant cell walls. – Biopolymers 39: 51–66.

Ha, M. A., Evans, B. W., Jarvis, M. C., Apperley, D. C. & Kenwright, A. M. 1996. CP-MAS NMR of highly mobile hydrated biopolymers – polysaccharides of *Allium* cell walls. – Carbohydr. Res. 288: 15–23.

Iraki, N. M., Bressan, R. A., Hasegawa, P. M. & Carpita, N. C. 1989a. Alteration of the physical and chemical structure of the primary cell wall of growth-limited plant cells adapted to osmotic stress. – Plant Physiol. 91: 39–47.

– , Singh, N., Bressan, R. A. & Carpita, N. C. 1989b. Cell walls of tobacco cells and changes in composition associated with reduced growth upon adaptation to water and saline stress. – Plant Physiol. 91: 48–53.

Kemsley, E. K., Belton, P. S., McCann, M. C., Ttofis, S., Wilson, R. H. & Delgadillo, I. 1994. A rapid method for the authentication of vegetable matter using Fourier Transform Infrared spectroscopy. – Food Control 5: 241–243.

Knox, J. P., Linstead, P. J., King, J., Cooper, C. & Roberts, K. 1990. Pectin esterification is spatially regulated both within cell walls and between developing tissues of root apices. – Planta 181: 512–521.

Lai, Y. W., Kemsley, E. K. & Wilson, R. H. 1994. Potential of Fourier Transform Infrared spectroscopy for the authentication of vegetable oils. – J. Agric. Food Chem. 42: 1154–1159.

McCann, M. C. & Roberts, K. 1991. Architecture of the primary cell wall. – *In* The Cytoskeletal Basis of Plant Growth and Form (C.W. Lloyd, ed.), pp. 109–129. Academic Press, New York, NY. ISBN 0-12-453770-7.

– & Roberts, K. 1994. Changes in cell wall architecture during cell elongation. – J. Exp. Bot. 45: 1683–1691.

– , Hammouri, M. K., Wilson, R. H., Belton, P. S. & Roberts, K. 1992. Fourier Transform Infra-Red microspectroscopy is a new way to look at plant cell walls. – Plant Physiol. 100: 1940–1947.

– , Stacey, N. J., Wilson, R. & Roberts, K. 1993. Orientation of macromolecules in the walls of elongating carrot cells. – J. Cell Sci. 106: 1347–1356.

– , Shi, J., Roberts, K. & Carpita, N. C. 1994. Changes in pectin structure and localisation during the growth of unadapted and NaCl-adapted tobacco cells. – Plant J. 5: 773–785.

– , Roberts, K., Wilson, R. H., Gidley, M. J., Gibeaut, D. M., Kim, J.-B. & Carpita, N. C. 1995. Old and new ways to probe plant cell-wall architecture. – Can. J. Bot. 73 (Suppl.): S103–S113.

Morikawa, H., Hayashi, R. & Senda, M. 1978. Infrared analysis of pea stem cell walls and oriented structure of matrix polysaccharides in them. – Plant Cell Physiol. 19: 1151–1159.

Mort, A., Moerschbacher, B. M., Pierce, M. L. & Maness, N. O. 1991. Problems encountered during the extraction, purification and chromatography of pectic fragments, and some solutions to them. – Carbohydr. Res. 215: 219–227.

Pennell, R. I &. Roberts, K. 1995. Monoclonal antibodies to cell-specific cell-surface carbohydrates in plant cell biology and development. – Methods Cell Biol. 49: 123–141.

Perkins, W. D. 1987. Fourier Transform-Infrared spectroscopy. Part II. Advantages of FT-IR. Topics in chemical instrumentation, Vol. 64, No. 11. – J. Chem. Educ. A269–271.

Redgwell, R. J. & Selvendran, R. R. 1986. Structural features of cell-wall polysaccharides of onion *Allium cepa*. – Carbohydr. Res. 157: 183–199.

Reiter, W.-D., Chapple, C. C. S. & Somerville, C. R. 1993. Altered growth and cell walls in a fucose-deficient mutant of *Arabidopsis*. – Science 261: 1032–1035.

Sene, C. F. B., McCann, M. C., Wilson, R. H. & Grinter, R. 1994. FT-Raman and FT-Infrared spectroscopy: An investigation of five higher plant cell walls and their components. – Plant Physiol. 106: 1623–1633.

Shedletzky, E., Shmuel, M., Delmer, D. P. & Lamport, D. T. A. 1990. Adaptation and growth of tomato cells on the herbicide 2,6-dichlorobenzonitrile leads to production of unique cell walls virtually lacking a cellulose-xyloglucan network. – Plant Physiol 94: 980–987.

Steele, N. M., McCann, M. C. & Roberts, K. 1997. Pectin modification in cell walls of ripening tomatoes occurs in distinct domains. – Plant Physiol. 114: 1–9.

Sutherland, G. B. B. M. 1952. Infrared analysis of the structure of amino acids, polypeptides and proteins. – Biochim. Biophys. Acta 6: 291–318.

Wells, B., McCann, M. C., Shedletzky, E., Delmer, D. & Roberts, K. 1994. Structural features of cell walls from tomato cells adapted to grow on the herbicide 2,6-dichlorobenzonitrile. – J. Microsc. 173: 155–164.

Williams, D. H. & Fleming, I. (eds). 1980. Spectroscopic Methods in Organic Chemistry, 3rd Ed., pp. 35–73. – McGraw Hill, New York, NY. ISBN 0-07-084108-X.

Wilson, R. H. 1990. Fourier transform mid-infrared spectroscopy for food analysis. – Trends Anal. Chem. 9: 127–131.

Edited by C. H. Bornman